ELSEVIER

Generalized principal component beamformer for communication systems

Mehrzad Biguesh[a,*], Shahrokh Valaee[b], Benoît Champagne[c]

[a]*Department of Communication Engineering, Duisburg-Essen University, Bismarckstrasse 81, 47057 Duisburg, Germany*
[b]*Department of ECE, University of Toronto, 10 King's College Road, Toronto, Canada M5S 3G4*
[c]*Department of ECE, McGill University, 3480 University Street, Montreal, Canada H3A 2A7*

Abstract

The contribution of this paper is two-fold. First, we introduce a generalized principal component (GPC) beamforming technique for reduced rank processing that allows a trade-off between interference and noise reduction via the introduction of a control parameter, ε. Three variants of the GPC beamformer corresponding to $\varepsilon = 1$ (called T1 beamformer), $\varepsilon = 0.5$ (called T2 beamformer) and $\varepsilon = 0$ (called T3 beamformer), which maximize the signal-to-interference ratio, the signal-to-interference plus noise ratio, and the signal-to-noise ratio at the array output respectively, are considered in detail. The second contribution of this paper is to compare the robustness between the reduced rank and full rank beamformers. We use analytical studies and computer simulations to show that the T2 and T3 beamformers are robust against calibration and/or pointing errors.
© 2004 Elsevier B.V. All rights reserved.

Keywords: Beamformer; Antenna array; Sidelobe canceller

1. Introduction

Extraction of a desired signal buried in noise and interference is of great importance. The use of an antenna array, with a properly selected weight vector, has long been recognized as a method to mitigate the destructive effect of interference and noise to efficiently extract the desired signal. In the array processing literature, several algorithms have been proposed that maximize the array output signal-to-interference plus noise ratio (SINR) subject to knowing the direction-of-arrival (DOA) of the desired signal; see for instance, the multiple sidelobe canceller (MSC) and the minimum variance (MV) methods [15]. In these cases, the weight vector is in effect computed from the signal-free correlation matrix (SFCM). One can also use the correlation matrix of the received

*Corresponding author. Tel.: +49 203 379 4390; fax: +49 203 379 2902.

E-mail addresses: biguesh@sent5.uni-duisburg.de (M. Biguesh), valaee@comm.utoronto.ca (S. Valaee), champagne@ece.mcgill.ca (B. Champagne).

mixture of signal, noise and interferences, and obtain the same result, provided the desired signal DOA and the array geometry are exactly known, and the antenna array is perfectly calibrated. Small errors in calibration and/or DOA estimation will cause signal cancellation [1,6].

In practice, the measurement of a SFCM is not a simple task, so that noise and interference are usually mixed with the signal. In radar applications, the SFCM may be estimated from the samples of the target adjacent range cells [5]. To estimate an SFCM, one can also use the generalized sidelobe canceller (GSC) [5,13]. In GSC, a prefiltering stage is applied to reject the signal component from the received samples and then the SFCM is estimated at the output of this stage. In this method, however, calibration and/or pointing errors will cause a leakage of the signal component into the noise subspace, which degrades the performance of the method by inducing high sidelobe levels and/or reducing desired signal power. Diagonal loading has been proposed to avoid signal cancellation in MV beamformers [4]. However, this loading method only bounds the white noise gain and its performance varies between that of MV and the conventional beamformer.

Besides the above mentioned disadvantages, in some cases, the performance of detection and demodulation depends on the signal-to-interference ratio (SIR). For example, in spread spectrum communications, penetration of a smart jammer into the system may cause a destructive effect on the system performance. In modern CDMA based wireless communication systems (e.g., IS-95, CDMA2000, etc.), the overall capacity, measured in terms of the number of active users per cell, is indeed limited by the power level of multi-user interference [7]. In such cases, interference minimization is much more important than the overall noise plus interference reduction.

Subspace-based methods offer significant improvement in signal reconstruction when compared to the conventional beamforming methods. Specially, there exist eigenvalue decomposition (EVD) methods that effectively estimate and track the eigen-subspace of the received signal covariance matrix [2,16]. As a consequence, the beam-forming methods, which are based on the eigendecomposition of array correlation matrix, have been the focus of much research [3,6,8,11,12,17,19]. In [6], a signal subspace method is proposed for interference cancellation that extracts the desired signal with a searching method. This method can only cancel one jammer. Haimovich [8] suggests two types of eigen-cancellers that are based on the eigendecomposition of the received interference plus noise correlation matrix and are applicable to radar systems. A comparison of several reduced-rank processing techniques for adaptive array can be found in [19]. A beamforming technique, which uses one or more eigenvectors of the received signal plus interference covariance matrix, is proposed in [11]. In [17], a modified eigenspace-based algorithm which is robust against pointing error is presented. McWhorter [12] uses the dominant subspace of the sample covariance matrix to construct an adaptive beamformer in a non-stationary environment. Chang et al. [3] presents a beamforming method based on the generalized eigenspace-based (GEIB) technique.

Our contribution in this paper is two-fold. Firstly, we introduce a new beamforming method based on an extended version of the reduced-rank principal component beamformer [19]. The proposed method, which we call *generalized principal component* (GPC) beamformer, incorporates a control parameter ($0 \leqslant \varepsilon \leqslant 1$) that allows a proper trade-off between interference and noise cancellation. Secondly, both analytically and using computer simulations, we study the robustness of the introduced method for special cases of the proposed parameter ε.

We study the properties of the GPC beamformer for three special but important cases, i.e. $\varepsilon = 1$, $\varepsilon = 0.5$, and $\varepsilon = 0$. For $\varepsilon = 1$ (T1 beamformer), we show that the GPC method maximizes the signal-to-interference ratio (SIR), producing exact nulls in the interference directions. With $\varepsilon = 0.5$ (T2 beamformer), the GPC method, for a calibrated array with the exact knowledge of the desired signal DOA, is shown to be similar to an MV beamformer. For $\varepsilon = 0$ (T3 beamformer), we show that under exact knowledge of the array manifold, the GPC is similar to the conventional

beamformer. For an arbitrary value of $0 < \varepsilon < 1$, the GPC method maximizes a properly weighted measure of signal-to-interference plus noise ratio.

In our study of robustness, we introduce a suitable measure of array sensitivity to array steering vector uncertainties, and use it to study the robustness of the T2 and T3 beamformers. We show that T2 and T3 beamformers have smaller sensitivity compared to the MV and conventional beamformers, respectively. We conclude that T2 and T3 are robust beamformers.

Throughout the present work, matrices will be indicated by capital boldface letters and vectors by lower-case boldface letters.

2. Signal model

We assume an L-element array with arbitrary geometry illuminated by p uncorrelated, far-field narrowband signal wavefronts. It is assumed that the number of sources is smaller than the number of array elements, that is $p < L$. Let $\mathbf{x}(k) = [x_1(k), \ldots, x_L(k)]^{\mathrm{T}}$ denote the complex envelope representation of the data received by the array elements at the kth snapshot. Data vector $\mathbf{x}(k)$ can be expressed as

$$\mathbf{x}(k) = \mathbf{A}\mathbf{s}(k) + \mathbf{n}(k), \tag{1}$$

where

$$\mathbf{A} = [\mathbf{a}(\theta_1)\, \mathbf{a}(\theta_2) \cdots \mathbf{a}(\theta_p)], \tag{2}$$

$$\mathbf{s}(k) = [s_1(k)\, s_2(k) \cdots s_p(k)]^{\mathrm{T}}, \tag{3}$$

$$\mathbf{n}(k) = [n_1(k)\, n_2(k) \cdots n_L(k)]^{\mathrm{T}}. \tag{4}$$

Here, $\mathbf{n}(k)$ is the background noise, which is assumed to be a stationary zero-mean stochastic process, $s_i(k)$ is the ith zero-mean stationary signal impinging on the array from distinct direction θ_i, and the superscript T represents transposition. The noise is temporally and spatially white and is uncorrelated with the desired signal and interferers. The complex vector $\mathbf{a}(\theta)$ is the array steering vector defined as the array output for a planar wavefront arriving at the array from direction θ with a unit power at the array reference point. In the case of an array with arbitrary planar geometry, the lth element of the steering vector $\mathbf{a}(\theta)$—with the array phase center located at the origin—can be expressed as

$$[\mathbf{a}(\theta)]_l = \exp\left\{ \mathrm{j} \frac{2\pi r_l}{\lambda} \cos(\theta - \phi_l) \right\}, \tag{5}$$

where (r_l, ϕ_l) denotes the position of the lth element in polar coordinates and λ denotes the wavelength at the operating frequency.

Using (1), the autocorrelation matrix of the array output is given by

$$\mathbf{R} = E\{\mathbf{x}(k)\mathbf{x}^{\mathrm{H}}(k)\} = \mathbf{A}\mathbf{P}\mathbf{A}^{\mathrm{H}} + \sigma^2 \mathbf{I}_L, \tag{6}$$

where $\mathbf{P} = \mathrm{diag}(p_1, \ldots, p_p)$, is the diagonal signal correlation matrix, σ^2 is the noise power and $\mathbf{I}_L$ is the $L \times L$ identity matrix. Here, $E\{.\}$ represents the expected value, superscript H denotes Hermitian transposition and p_i is the received power of the ith signal source. The diagonal structure of $\mathbf{P}$ indicates uncorrelated sources. Since $\mathbf{P}$ is diagonal, we can write (6) as

$$\mathbf{R} = \sum_{i=1}^{p} p_i \mathbf{a}(\theta_i)\mathbf{a}^{\mathrm{H}}(\theta_i) + \sigma^2 \mathbf{I}_L. \tag{7}$$

The sample covariance matrix, for a window of N snapshots, is defined as [9]

$$\hat{\mathbf{R}} = \frac{1}{N} \sum_{i=0}^{N-1} \mathbf{x}(k-i)\mathbf{x}^{\mathrm{H}}(k-i). \tag{8}$$

The sample correlation matrix is a random matrix and for Gaussian $\mathbf{x}$, it will be Wishart distributed [14].

2.1. Eigen-decomposition of covariance matrix

For the positive-definite correlation matrix $\mathbf{R}$, one can find a set of eigenvalues $\{\lambda_i + \sigma^2\}$ and orthonormal eigenvectors $\{\mathbf{q}_i\}$ such that

$$\mathbf{R}\mathbf{q}_i = (\lambda_i + \sigma^2)\mathbf{q}_i \quad \text{for} \quad 1 \leqslant i \leqslant L. \tag{9}$$

We assume λ_i's are in decreasing order as

$$\lambda_1 \geqslant \cdots \geqslant \lambda_L, \tag{10}$$

where $\lambda_i = 0$ for $p < i \leqslant L$. Hereafter, we will use the following notations

$$\lambda_{\max} = \lambda_1 \quad \text{and} \quad \lambda_{\min} = \lambda_p, \tag{11}$$

$$\mathbf{\Lambda} = \mathrm{diag}(\lambda_1 + \sigma^2, \ldots, \lambda_p + \sigma^2, \sigma^2, \ldots, \sigma^2), \qquad (12)$$

$$\mathbf{\Lambda}_s = \mathrm{diag}(\lambda_1 + \sigma^2, \ldots, \lambda_p + \sigma^2), \qquad (13)$$

$$\mathbf{\Lambda}_n = \sigma^2 \mathbf{I}_{(L-p)}, \qquad (14)$$

$$\mathbf{Q} = [\mathbf{q}_1, \ldots, \mathbf{q}_p \,|\, \mathbf{q}_{p+1}, \ldots, \mathbf{q}_L] = [\mathbf{Q}_s \,|\, \mathbf{Q}_n]. \qquad (15)$$

It is well known that $\mathbf{Q}_s$ and $\mathbf{A}$ span the same space called the *signal subspace*; while the eigenvectors corresponding to the $(L-p)$ smallest eigenvalues, $\mathbf{Q}_n$, are orthogonal to $\mathbf{a}(\theta_i)$ for $1 \leqslant i \leqslant p$ and span the so-called *noise subspace*. Thus, we have

$$\mathbf{Q}_n^H \mathbf{A} = \mathbf{0}. \qquad (16)$$

The correlation matrix $\mathbf{R}$ and its inverse $\mathbf{R}^{-1}$ can also be expressed as (Karhunen–Loève expansion)

$$\mathbf{R} = \sum_{i=1}^{L} (\lambda_i + \sigma^2) \mathbf{q}_i \mathbf{q}_i^H = \mathbf{Q} \mathbf{\Lambda} \mathbf{Q}^H, \qquad (17)$$

$$\mathbf{R}^{-1} = \sum_{i=1}^{L} (\lambda_i + \sigma^2)^{-1} \mathbf{q}_i \mathbf{q}_i^H = \mathbf{Q} \mathbf{\Lambda}^{-1} \mathbf{Q}^H. \qquad (18)$$

2.2. Properties of eigen-decomposition

Since $\mathbf{A}$ and $\mathbf{Q}_s$ both belong to the signal subspace, each $\mathbf{a}_i = \mathbf{a}(\theta_i)$ can be written as a linear combination of the $\mathbf{q}_j$'s (for $1 \leqslant j \leqslant p$), that is

$$[\mathbf{a}_1 \cdots \mathbf{a}_p] = [\mathbf{q}_1 \cdots \mathbf{q}_p] \begin{bmatrix} k_{11} & \cdots & k_{1p} \\ \vdots & & \vdots \\ k_{p1} & \cdots & k_{pp} \end{bmatrix}. \qquad (19)$$

In matrix form, (19) is given by

$$\mathbf{A} = \mathbf{Q}_s \mathbf{K}. \qquad (20)$$

Since the $\mathbf{q}_i$'s are orthonormal, we have

$$\mathbf{a}_i^H \mathbf{q}_j = k_{ji}^* \qquad (21)$$

or equivalently, in matrix form,

$$\mathbf{A}^H \mathbf{Q}_s = \mathbf{K}^H. \qquad (22)$$

The following lemmas express some important relationships for k_{ji}.

Lemma 1. *The Euclidean norm of any column of* $\mathbf{K}$, $\mathbf{k}_i$, *is equal to* L, *that is for* $1 \leqslant i \leqslant p$,

$$||\mathbf{k}_i||^2 = \sum_{j=1}^{p} |k_{ji}|^2 = L. \qquad (23)$$

Proof. Using (5), (19), and the orthonormality of eigenvectors, we have for $1 \leqslant i \leqslant p$,

$$\mathbf{a}_i^H \mathbf{a}_i = L,$$

$$(k_{1i} \mathbf{q}_1 + \cdots + k_{pi} \mathbf{q}_p)^H (k_{1i} \mathbf{q}_1 + \cdots + k_{pi} \mathbf{q}_p) = L,$$

$$\sum_{j=1}^{p} |k_{ji}|^2 = L. \qquad \square \qquad (24)$$

Lemma 2. *The inner product of any two columns of* $\mathbf{K}$ *is equal to the inner product of the corresponding columns of* $\mathbf{A}$,

$$\mathbf{k}_m^H \mathbf{k}_n = \sum_{i=1}^{p} k_{im}^* k_{in} = \mathbf{a}_m^H \mathbf{a}_n. \qquad (25)$$

Proof. Using (19), we have

$$\mathbf{a}_m^H \mathbf{a}_n = (k_{1m} \mathbf{q}_1 + \cdots + k_{pm} \mathbf{q}_p)^H (k_{1n} \mathbf{q}_1 + \cdots + k_{pn} \mathbf{q}_p)$$

$$= \sum_{i=1}^{p} k_{im}^* k_{in} = \mathbf{k}_m^H \mathbf{k}_n. \qquad \square$$

Lemma 3. *The columns of* $\mathbf{K}(\mathbf{\Lambda}_s - \sigma^2 \mathbf{I}_p)^{-1/2}$ *are orthogonal to each other and*

$$\sum_{i=1}^{p} k_{in}^* k_{im} / \lambda_i = \delta_{nm} / p_n. \qquad (26)$$

Proof. Using (7), (9) and (21), one gets for $1 \leqslant j \leqslant p$

$$\mathbf{R} \mathbf{q}_j = (\lambda_j + \sigma^2) \mathbf{q}_j$$

$$\longrightarrow \sum_{i=1}^{p} p_i \mathbf{a}_i \mathbf{a}_i^H \mathbf{q}_j = \lambda_j \mathbf{q}_j,$$

$$\longrightarrow \sum_{i=1}^{p} (p_i k_{ji}^* / \lambda_j) \mathbf{a}_i = \mathbf{q}_j. \qquad (27)$$

Write (27) as

$$\mathbf{A} \tilde{\mathbf{K}} = \mathbf{Q}_s, \qquad (28)$$

where $\tilde{\mathbf{K}}$ is defined as

$$\tilde{\mathbf{K}} = \begin{bmatrix} \frac{p_1 k_{11}^*}{\lambda_1} & \cdots & \frac{p_1 k_{p1}^*}{\lambda_p} \\ \vdots & & \vdots \\ \frac{p_p k_{1p}^*}{\lambda_1} & \cdots & \frac{p_p k_{pp}^*}{\lambda_p} \end{bmatrix} = \mathbf{P}\mathbf{K}^{\mathrm{H}}(\mathbf{\Lambda}_s - \sigma^2 \mathbf{I}_p)^{-1}.$$

(29)

Since it is assumed that $\mathbf{A}$ is full column rank, and using (20) and (28), we have

$$\tilde{\mathbf{K}}\mathbf{K} = \mathbf{I}_p.$$

(30)

Thus, the nmth element of $\tilde{\mathbf{K}}\mathbf{K}$ may be written as

$$\sum_{i=1}^{p} p_n \frac{k_{in}^* k_{im}}{\lambda_i} = \delta_{nm}$$

(31)

and the proof is completed. $\square$

Lemma 4. *The rows of $\mathbf{K}\mathbf{P}^{1/2}$ are orthogonal to each other and*

$$\sum_{i=1}^{p} p_i k_{ni} k_{mi}^* = \lambda_m \delta_{nm}.$$

(32)

Proof. Using (28) and (20), yields

$$\mathbf{K}\tilde{\mathbf{K}} = \mathbf{I}_p.$$

(33)

The nmth element of $\mathbf{K}\tilde{\mathbf{K}}$ will then be

$$\sum_{i=1}^{p} p_i k_{ni} k_{mi}^* = \lambda_m \delta_{nm}. \qquad \square$$

(34)

Lemmas 3 and 4 can also be expressed in the following matrix forms,

$$\mathbf{K}^{\mathrm{H}}(\mathbf{\Lambda}_s - \sigma^2 \mathbf{I}_p)^{-1}\mathbf{K} = \mathbf{P}^{-1},$$

(35)

$$\mathbf{K}\mathbf{P}\mathbf{K}^{\mathrm{H}} = (\mathbf{\Lambda}_s - \sigma^2 \mathbf{I}_p).$$

(36)

In the sequel, we will use the above results to study the characteristics of the GPC beamformer.

3. GPC beamformer

We propose to find the beamforming weight vector $\mathbf{w}$ in order to maximize the following

ratio

$$\mathbf{w}_{n,\varepsilon} = \max_{\mathbf{w}} \frac{S_{\mathrm{o}}}{\varepsilon I_{\mathrm{o}} + (1 - \varepsilon)N_{\mathrm{o}}} \quad \text{for } 0 \leqslant \varepsilon \leqslant 1, \quad (37)$$

where S_{o}, I_{o} and N_{o}, which are functions of weight vector $\mathbf{w}$, respectively denote the signal power due to nth source, the total interference power, and the noise power at the array output. To maximize the ratio (37), one can equivalently solve the following optimization problem,

$$\min_{\mathbf{w}} \varepsilon S_{\mathrm{o}} + \varepsilon I_{\mathrm{o}} + (1 - \varepsilon)N_{\mathrm{o}} \quad \text{subject to } S_{\mathrm{o}} = c,$$

(38)

where, c is some positive constant.

Assuming that the nth point source is the desired one, $S_{\mathrm{o}} = p_n |\mathbf{a}_n^{\mathrm{H}} \mathbf{w}|^2$. The solution to (38) can be obtained using the Lagrange multiplier method by means of minimizing,

$$\begin{aligned} L(\mathbf{w}, \lambda) = {}& \varepsilon S_{\mathrm{o}} + \varepsilon I_{\mathrm{o}} + (1 - \varepsilon)N_{\mathrm{o}} \\ & - \lambda(\sqrt{p_n}\mathbf{a}_n^{\mathrm{H}}\mathbf{w} - \sqrt{c}). \end{aligned}$$

(39)

Putting $\partial L(\mathbf{w}, \lambda)/\partial \mathbf{w} = 0$, taking into account that $S_{\mathrm{o}} + I_{\mathrm{o}} = \mathbf{w}^{\mathrm{H}}(\mathbf{R} - \sigma^2 \mathbf{I})\mathbf{w}$, and ignoring a constant coefficient, it is straightforward to show that

$$\mathbf{w}_{n,\varepsilon} = (\varepsilon \mathbf{R} + (1 - 2\varepsilon)\sigma^2 \mathbf{I})^{-1}\mathbf{a}_n.$$

(40)

Now, with the assumption that the other $p - 1$ interferers are also point sources, we can use (17) and (16), to write (40) in terms of signal subspace eigen-pairs (i.e. $(\lambda_i, \mathbf{q}_i)$ for $i = 1, \ldots, p$).

$$\mathbf{w}_{n,\varepsilon} = \sum_{i=1}^{p} \frac{\mathbf{q}_i \mathbf{q}_i^{\mathrm{H}}}{\varepsilon \lambda_i + (1 - \varepsilon)\sigma^2} \mathbf{a}_n, \quad \text{for } 0 \leqslant \varepsilon \leqslant 1. \quad (41)$$

Considering the reduced-rank principal component beamformer[1] [19], which corresponds to the case $\varepsilon = 0.5$, we call (41) the GPC beamformer (where several beamformers are formed by varying ε, thereby extending the original PC scheme in [19]) to compute the beamforming weights.

Here, our main goal is to study the properties of this beamformer for three different values of ε (that is $\varepsilon = 1$, 0.5, 0).

---

[1]Some authors call it the generalized eigenspace-based (GEIB) beamformer or the eigenspace-based (ESB) beamformer [10,18].

3.1. Type-1 (T1) beamformer

For this beamformer, we use $\varepsilon = 1$ in (41) and compute the beamformer weight vector as

$$\mathbf{w}_{n,1} = \sum_{i=1}^{p} \frac{\mathbf{q}_i \mathbf{q}_i^{\mathrm{H}}}{\lambda_i} \mathbf{a}_n = \mathbf{Q}_s(\mathbf{\Lambda}_s - \sigma^2 \mathbf{I}_p)^{-1} \mathbf{Q}_s^{\mathrm{H}} \mathbf{a}_n. \qquad (42)$$

The set of beamformer weight vectors for all signals can be represented as

$$\mathbf{W}_1 = [\mathbf{w}_{1,1} \cdots \mathbf{w}_{p,1}] = \mathbf{Q}_s(\mathbf{\Lambda}_s - \sigma^2 \mathbf{I}_p)^{-1} \mathbf{Q}_s^{\mathrm{H}} \mathbf{A}. \qquad (43)$$

Theorem 1. *The pattern of* T1 *beamformer has nulls in the direction of interferers and its gain in the direction of the desired signal is equal to the inverse of the received power from the target source.*

Proof. The array gain in the direction θ_m is generally expressed as $\mathbf{a}_m^{\mathrm{H}} \mathbf{w}_{n,\varepsilon}$. Using (21), (42), and Lemma 3, we can proceed as follows:

$$\mathbf{a}_m^{\mathrm{H}} \mathbf{w}_{n,1} = \sum_{i=1}^{p} \mathbf{a}_m^{\mathrm{H}} \frac{\mathbf{q}_i \mathbf{q}_i^{\mathrm{H}}}{\lambda_i} \mathbf{a}_n = \sum_{i=1}^{p} \frac{k_{im}^* k_{in}}{\lambda_i} = \frac{\delta_{nm}}{p_n}. \qquad (44)$$

Using (22) and (35) in matrix form, we have

$$\begin{aligned}\mathbf{A}^{\mathrm{H}} \mathbf{W}_1 &= \mathbf{A}^{\mathrm{H}} \mathbf{Q}_s(\mathbf{\Lambda}_s - \sigma^2 \mathbf{I}_p)^{-1} \mathbf{Q}_s^{\mathrm{H}} \mathbf{A} \\ &= \mathbf{P}^{-1} = \mathrm{diag}(p_1^{-1}, \dots, p_p^{-1}).\end{aligned} \qquad (45)$$

From (44) and (45), it is seen that the array produces exact nulls in the direction of interference (that is for θ_m whenever $m \neq n$), and the array gain in the direction of the desired source is equal to the inverse of the received signal power p_n^{-1}. □

Since the T1 beamformer produces exact nulls in the direction of interferences, the output interference power for this beamformer is zero. In other words, this weight vector maximizes the array output SIR. Accordingly, the output SNR and output SINR are identical.

The desired signal power at the array output, say S_{o}, is equal to the desired source power, p_n, multiplied by the array power gain in the direction of the desired signal. Therefore:

Corollary 1. *The output power of the desired signal,* S_{o}, *is*

$$S_{\mathrm{o}} = p_n |\mathbf{a}_n^{\mathrm{H}} \mathbf{w}_{n,1}|^2 = p_n \left| \frac{1}{p_n} \right|^2 = \frac{1}{p_n}. \qquad (46)$$

Theorem 2. *For the* T1 *beamformer, the output SNR is bounded by* $\lambda_{\min}/\sigma^2$ *and* $\lambda_{\max}/\sigma^2$.

Proof. Using (21), (42), and the orthonormality of $\mathbf{q}_i$'s, the array output noise power, N_{o}, is

$$N_{\mathrm{o}} = \sigma^2 \mathbf{w}_{n,1}^{\mathrm{H}} \mathbf{w}_{n,1} = \sigma^2 \sum_{i=1}^{p} \frac{|k_{in}|^2}{\lambda_i^2}. \qquad (47)$$

Using (46), (47), and Lemma 3, we have

$$\frac{\sigma^2}{\lambda_{\max}} \sum_{i=1}^{p} \frac{|k_{in}|^2}{\lambda_i} \leqslant S_{\mathrm{o}} \leqslant \frac{\sigma^2}{\lambda_{\min}} \sum_{i=1}^{p} \frac{|k_{in}|^2}{\lambda_i},$$

$$\frac{1}{p_n}\left(\frac{\sigma^2}{\lambda_{\max}}\right) \leqslant N_{\mathrm{o}} \leqslant \frac{1}{p_n}\left(\frac{\sigma^2}{\lambda_{\min}}\right),$$

$$\frac{\lambda_{\min}}{\sigma^2} \leqslant \frac{S_{\mathrm{o}}}{N_{\mathrm{o}}} \leqslant \frac{\lambda_{\max}}{\sigma^2}. \qquad □ \qquad (48)$$

3.2. Type-2 (T2) beamformer

For this beamformer, we use $\varepsilon = 0.5$ in (41) and obtain[2]

$$\mathbf{w}_{n,0.5} = \sum_{i=1}^{p} \frac{\mathbf{q}_i \mathbf{q}_i^{\mathrm{H}}}{\lambda_i + \sigma^2} \mathbf{a}_n = \mathbf{Q}_s \mathbf{\Lambda}_s^{-1} \mathbf{Q}_s^{\mathrm{H}} \mathbf{a}_n, \qquad (49)$$

which is the weight vector for the conventional reduced-rank principal component method [19]. Using the Karhunen–Loève expansion, (17), and (16), the following relationship—the minimum variance (MV) solution for the array weight vector—can be obtained

$$\mathbf{w}_{n,0.5} = \mathbf{R}^{-1} \mathbf{a}_n. \qquad (50)$$

A shortcoming of the MV beamformer is its sensitivity to signal DOA uncertainty and array calibration error [4]. We will see in the sequel that

---

[2]In (49), a coefficient 0.5 in the denominator has been dropped for simplicity.

the T2 beamformer is less sensitive to these errors when compared to the MV technique.

Definition. For an array with the weight vector $\mathbf{w}$, we define the sensitivity of array output SINR with respect to the array steering vector error $(\Delta \mathbf{a} = \tilde{\mathbf{a}} - \mathbf{a})$ as[3]

$$\mathcal{S}_{\text{SINR}_o,\mathbf{a}}^{\mathbf{w}} = \lim_{\Delta \mathbf{a} \to 0} \frac{|\Delta \text{SINR}_o|}{||\Delta \mathbf{a}||^2}, \tag{51}$$

where $\Delta \text{SINR}_o = \text{SINR}_o|_{\Delta \mathbf{a}=0} - \text{SINR}_o|_{\Delta \mathbf{a} \neq 0}$. Now, we use (51), as a novel and suitable measure of beamformer sensitivity to array steering vector errors, to show the robustness of T2 beamformer.

Theorem 3. *The sensitivity of output SINR to the array steering vector error in* T2 *beamformer is smaller than that for* MV.

Proof. See Appendix A. $\quad\square$

3.3. Type-3 (T3) beamformer

For this reduced-rank beamformer, we use (41) with $\varepsilon = 0$. The corresponding weight vector is

$$\mathbf{w}_{n,0} = \sum_{i=1}^{p} \frac{\mathbf{q}_i \mathbf{q}_i^{\text{H}}}{\sigma^2} \mathbf{a}_n = \frac{1}{\sigma^2} \mathbf{Q}_s \mathbf{Q}_s^{\text{H}} \mathbf{a}_n. \tag{52}$$

Knowing that $\mathbf{Q}_n^{\text{H}} \mathbf{A} = \mathbf{0}$ and $\mathbf{Q}_s \mathbf{Q}_s^{\text{H}} = \mathbf{I}_L - \mathbf{Q}_n \mathbf{Q}_n^{\text{H}}$, (52) can be written as

$$\mathbf{w}_{n,0} = \frac{1}{\sigma^2} \mathbf{a}_n, \tag{53}$$

which is the well-known conventional beamformer (note that (52) and (53) are identical if $\mathbf{a}_n$ is exactly known, otherwise they are different). Accordingly, the T3 beamformer maximizes the output SNR. However, as we shall show, the T3 beamformer is less sensitive than the conventional beamformer to steering vector errors. Using (53), it is straightforward to compute the output SNR as

$$\text{SNR}_o = p_n \frac{\mathbf{a}_n^{\text{H}} \mathbf{a}_n}{\sigma^2}, \tag{54}$$

which is independent of the number of sources p.

---

[3]The steering vector mismatch $(\tilde{\mathbf{a}} \neq \mathbf{a})$ may be due to system calibration error, pointing error, and/or unsynchronized A/D converters.

Definition. For an array with the weight vector $\mathbf{w}$, we define the sensitivity of array output SNR with respect to the array steering vector error $(\Delta \mathbf{a} = \tilde{\mathbf{a}} - \mathbf{a})$ as

$$\mathcal{S}_{\text{SNR}_o,\mathbf{a}}^{\mathbf{w}} = \lim_{\Delta \mathbf{a} \to 0} \frac{|\Delta \text{SNR}_o|}{||\Delta \mathbf{a}||^2}, \tag{55}$$

where $\Delta \text{SNR}_o = \text{SNR}_o|_{\Delta \mathbf{a}=0} - \text{SNR}_o|_{\Delta \mathbf{a} \neq 0}$.

Theorem 4. *The sensitivity of output SNR of* T3 *beamformer to the array steering vector error is smaller than that for the conventional beamformer.*

Proof. See Appendix B. $\quad\square$

For the T3 beamformer, the array output signal and noise power, using (53), can be computed as

$$S_o = p_n |\mathbf{a}_n^{\text{H}} \mathbf{w}_{n,0}|^2 = p_n \frac{1}{\sigma^4} L^2, \tag{56}$$

$$N_o = \sigma^2 \mathbf{w}_{n,0}^{\text{H}} \mathbf{w}_{n,0} = \frac{1}{\sigma^2} L. \tag{57}$$

Dividing (56) by (57), the array output SNR can be expressed in terms of input SNR as

$$\frac{S_o}{N_o} = L \frac{p_n}{\sigma^2} = L \left(\frac{S}{N} \right)_{\text{in}}. \tag{58}$$

4. Simulation results

This section presents some numerical results to illustrate the performance of the proposed GPC approach. Here, all sources have unit power and are uniformly distributed in $[0°, 360°]$. Ten thousand Monte-Carlo runs are performed to calculate each point in the simulations. We assume that the additive noise is spatially and temporally white. Additionally, we assume that the true correlation matrix is known. To investigate the performance of the proposed method, an 8-element uniform circular array (UCA), with the inter-element spacing $\lambda/2$, was considered.

Fig. 1 shows typical patterns produced with the beamformer $\mathbf{w}_{n,\varepsilon}$ (41) for $\varepsilon = 1, 0.5, 0.2, 0.1, 0.05$. The interference is generated by two point sources located at angles $76°$ and $236°$. The desired signal DOA is at $180°$. The figure shows the changes in beampattern with ε as expected from the above
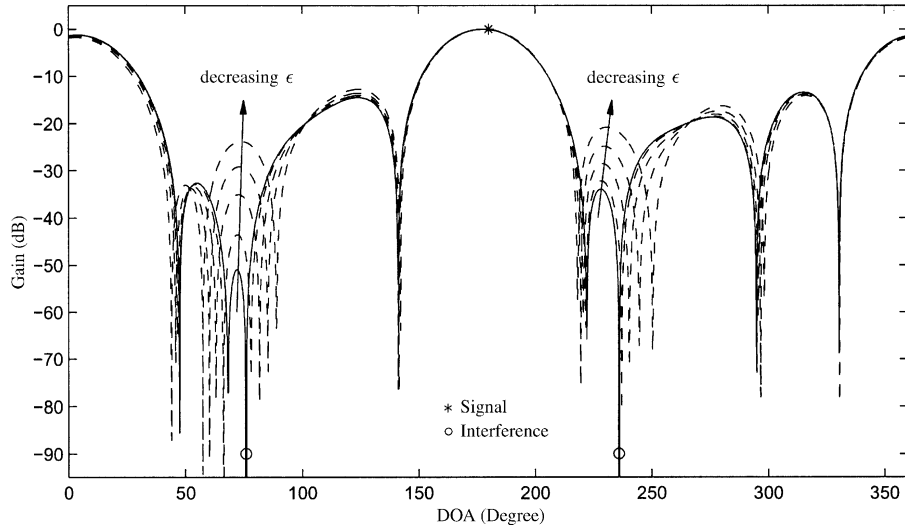
Fig. 1. Produced beampatterns using GPC beamformers method ($\varepsilon = 1$, 0.5, 0.2, 0.1, 0.05).

analysis. Note the deep nulls in the direction of interferers for large values of ε.

Fig. 2 illustrates the effect of ε on the array output SINR, SNR, and SIR for up to seven sources (i.e. $p = 2, \ldots, 7$), where sources have 10 dB signal-to-noise ratio. These figures illustrate how the array output SINR, SNR and SIR vary with the parameter ε. Specially, for this example, the maximum output SIR, SINR and SNR occur respectively at $\varepsilon = 1$, $\varepsilon = 0.5$, and $\varepsilon = 0$, which agrees with our analytical studies in Section 3. The observed high SIR at the output for large value of ε is due to the presence of exact nulls in the direction of interfering sources. According to the simulation results, it is seen that for larger values of p, SNR may experience large variations versus ε. This may be explained by the larger dimension of the signal subspace, where as a result, the GPC beamformer (41) will pass more noise in its output when ε is not properly tuned for optimum noise rejection. The curves in Fig. 2 show that the output SINR, SNR and SIR decrease with p. However, as suggested by (54), for $\varepsilon = 0$, the output SNR is independent of the number of interferers.

In Section 3.2, it has been proved that the array output SINR for the T2 beamformer is less sensitive to calibration or pointing error as compared to the MV beamformer. To investigate this aspect, we define RS_1, a measure for relative sensitivity, as

$$RS_1 = \mathscr{S}_{\mathrm{SINR_o}}^{\mathbf{w}_{m,0.5}} / \mathscr{S}_{\mathrm{SINR_o}}^{\mathbf{w}_{m,MV}}, \tag{59}$$

Fig. 3 illustratesthis relative sensitivity as a function of the received noise power for different values of p. The curves indicate that the T2 beamformer is robust for the steering vector estimation errors when compared to the MV method, specially for high SNR and small p.

Similarly, we define RS_2 as

$$RS_2 = \mathscr{S}_{\mathrm{SNR_o}}^{\mathbf{w}_{m,0}} / \mathscr{S}_{\mathrm{SNR_o}}^{\mathbf{w}_{m,C}}, \tag{60}$$

where $\mathbf{w}_{m,C}$ is the weight vector of the conventional beamformer. Fig. 4 shows RS_2 versus received noise power for different values of p. The sensitivity of T3 is smaller than that of the conventional beamformer, as evidenced by values $RS_2 < 1$. The curves show that the relative sensitivity is independent of the input SNR. Indeed, according to (70) and (71), sensitivities of T3 and the conventional beamformer are linear functions of input SNR. Hence, the relative sensitivity RS_2 will be independent of input SNR. Finally, referring to (62), (70) and (71), as we might have expected, RS_2 approaches unity with increasing p.

Although all array elements are assumed to be identical omni-directional elements, in practice, element imperfection and mutual coupling can cause both phase and amplitude distortion.
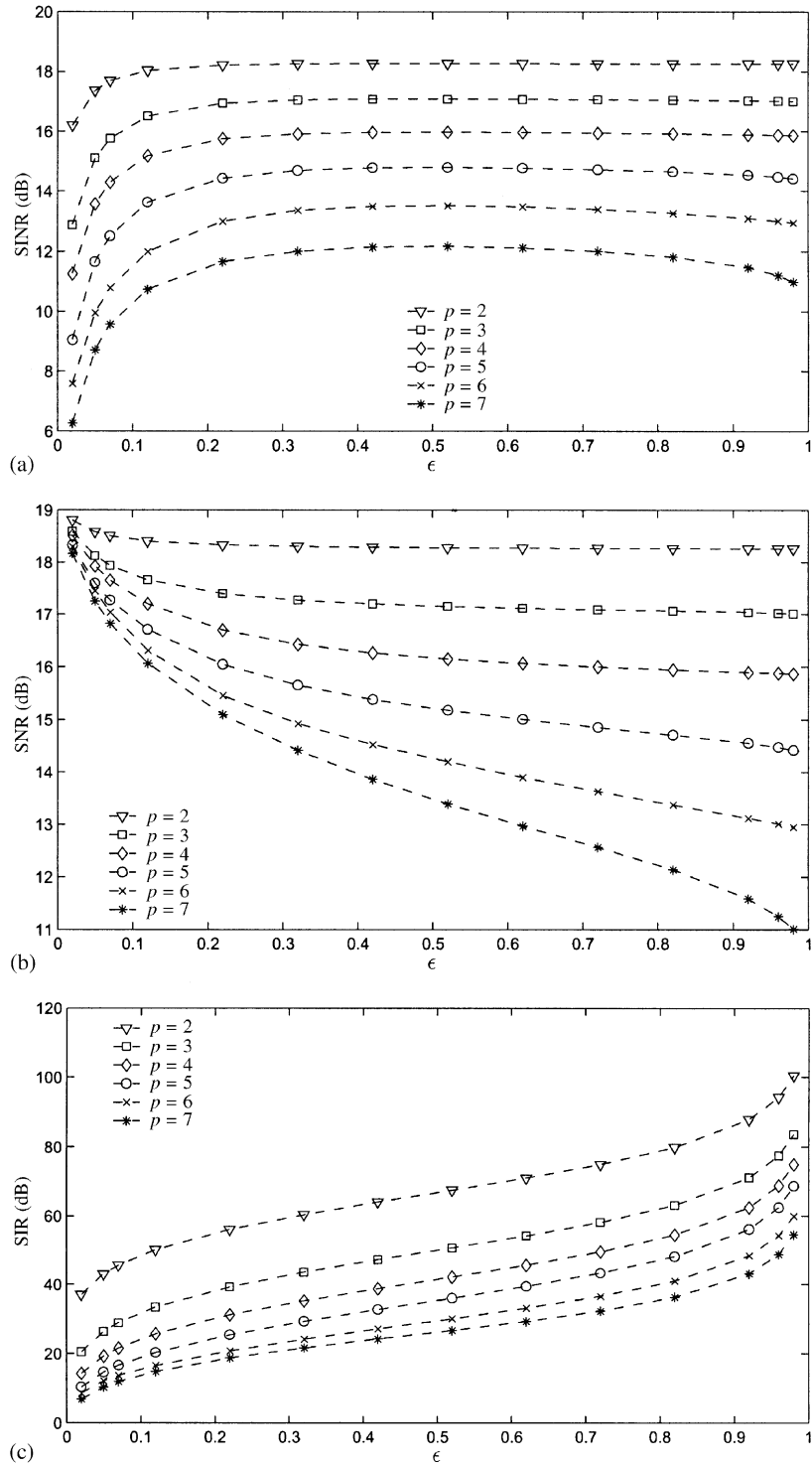
Fig. 2. Array output SINR, SNR and SIR as a function of ε for $p = 2, 3, \ldots, 7$.
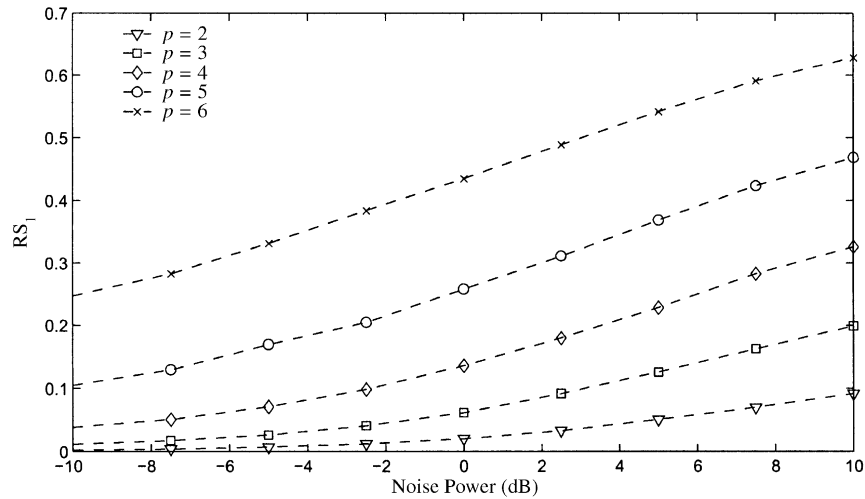
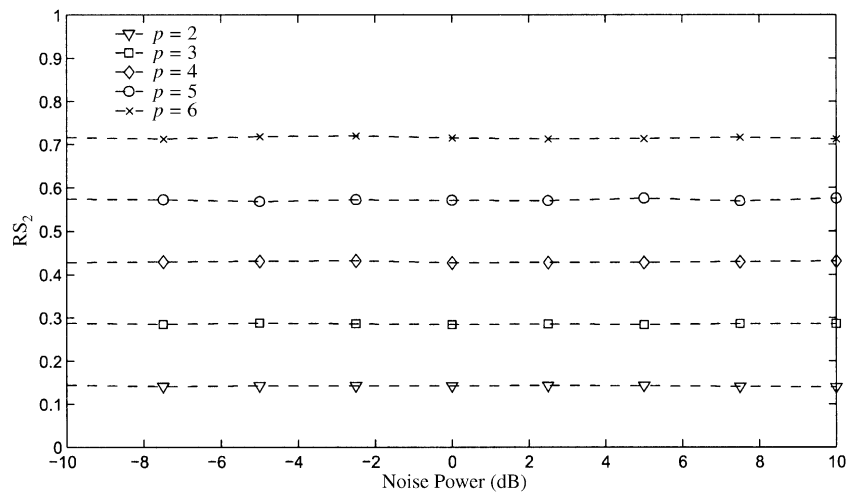Fig. 3. RS_1 versus the input SNR for $p = 2, 3, 4, 5, 6$.

Fig. 4. RS_2 versus the input SNR for $p = 2, 3, 4, 5, 6$.

Furthermore, different length of transmission lines, phase error at the local oscillator and mixer of the antenna elements and synchronization error of A/D converters in digital beamformers are sources of phase error of an adaptive beamformer. Practically, these errors cause degradation in the performance of beamforming algorithms.

Fig. 5 demonstrates the destructive effect of the phase error on the proposed GPC method by illustrating the output SINR, SNR and SIR as a function of ε and ϕ_{max} where ϕ_{max} is the maximum phase error of array elements. In this example, the input SNR is assumed to be 10 dB, $p = 6$, and the array elements experience fixed independent random phase errors. As seen, the beamformer performance is less affected by the phase errors for small values of ε. Regarding Fig. 5(a), we also note that in order to achieve good SINR performance in the presence of phase and/or angle errors, one needs to trade-off interference for noise suppression via a different choice of ε, specifically for $\varepsilon < 0.5$. According to the simulation results, the phase errors may be regarded as an increase in the noise power; consequently, the SINR is maximized for a lower ε. Note that for this scenario the array output SINR when MV beamformer is used are
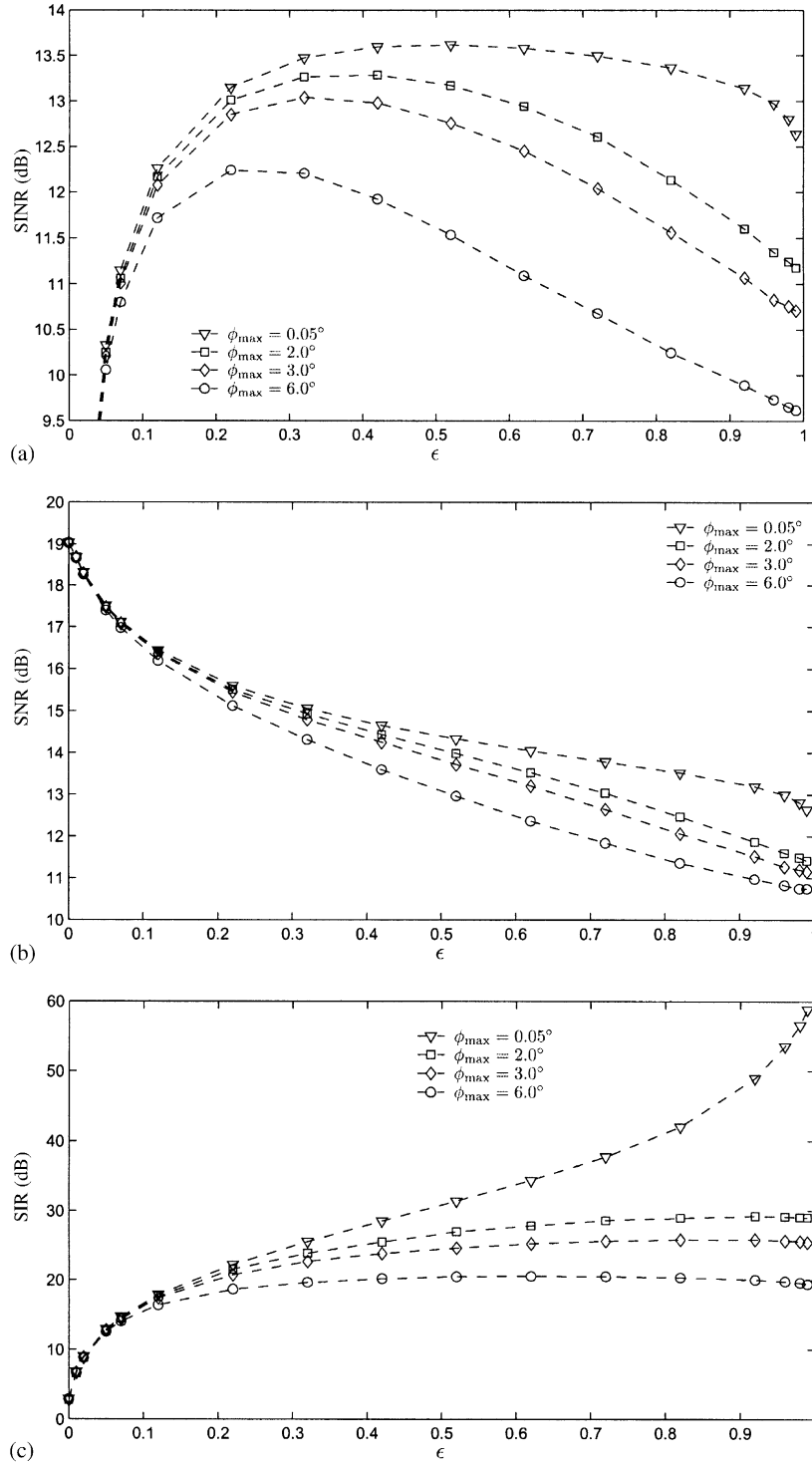
Fig. 5. Array output SINR, SNR and SIR as a function of ε for $\phi_{\max} = 0.05°, 2°, 3°$, and $6°$.

13.6, 12.2, 11.1, and 8.1 dB for $\phi_{max} = 0.05°, 2°, 3°,$ and $6°$, respectively.

A similar situation prevails for SIR where the optimal choice of ε may be less than 1 for larger phase errors. Based on these experimental results, we conclude that one may use the GPC method to make the beamformer robust against calibration errors; i.e. one can maximize the output SINR or SIR by proper choice of the parameter ε.

5. Conclusion

In this paper, we have proposed the GPC beamformer which can be used with arbitrary array geometries. The GPC beamforming technique uses the signal subspace eigenvalues and eigenvectors of the array correlation matrix. The weight vector of the beamformer is a weighted combination of the signal eigenvectors and is parameterized with respect to a variable, ε.

We have discussed the GPC beamformer with three values for ε —namely T1 ($\varepsilon = 1$), T2 ($\varepsilon = 0.5$), and T3 ($\varepsilon = 0$) beamformers. It has been shown that T2 and T3 coincide, respectively, with the MV and conventional beamformers provided that the exact location of the desired signal is known and the calibration error is absent. We have shown with simulations that T2 beamformer outperforms MV method if the scenario under test suffers from calibration errors and/or DOA uncertainty.

With the recent advances in the area of fast subspace tracking algorithms, the computational complexity of signal subspace eigenvalues and eigenvectors estimation and tracking can now be reduced to $O(pL)$ operations per time iteration [2,16]. While the main advantage of the proposed GPC method remains its robustness against different types of modelling errors, the use of such fast EVD tracking algorithms makes it computationally efficient for adaptive beamforming in dynamic signal environments.

Although falling outside the scope of the present work, the possibility of optimizing the method with respect to the choice of ε (e.g. based on application specific penalty function) remains open for future work.

Appendix A. Proof of Theorem 3

The array output SINR is

$$\text{SINR}_o = \frac{p_m G(\theta_m)}{N + \sum_{i \neq m} p_i G(\theta_i)}, \tag{61}$$

where $G(\theta)$ is the array power gain in the direction θ, and θ_m is the desired signal DOA. Now, assume that there is an uncertainty in $\mathbf{a}_m$ and represent its erroneous estimate by $\tilde{\mathbf{a}}_m$. The estimated $\tilde{\mathbf{a}}_m$ can be shown as a linear combination of the signal and noise eigenvectors as

$$\tilde{\mathbf{a}}_m = \mathbf{a}_m + \Delta \mathbf{a}_m = \mathbf{Q}_s \mathbf{k}_m + \mathbf{Q}_s \Delta \mathbf{k}_{ms} + \mathbf{Q}_n \Delta \mathbf{k}_{mn}, \tag{62}$$

where $\Delta \mathbf{a}_m = [\mathbf{Q}_s | \mathbf{Q}_n][\Delta \mathbf{k}_{ms}^T, \Delta \mathbf{k}_{mn}^T]^T$, is the uncertainty in $\mathbf{a}_m$, and $\Delta \mathbf{k}_{ms}$ and $\Delta \mathbf{k}_{mn}$ represent respectively the signal and noise error vectors in the mth column of matrix $\mathbf{K}$.

The weight vectors for the T2 and MV beamformers are, respectively,

$$\tilde{\mathbf{w}}_{m,0.5} = \mathbf{Q}_s \mathbf{\Lambda}_s^{-1} \mathbf{Q}_s^H \tilde{\mathbf{a}}_m = \mathbf{Q}_s \mathbf{\Lambda}_s^{-1} \mathbf{k}_m + \mathbf{Q}_s \mathbf{\Lambda}_s^{-1} \Delta \mathbf{k}_{ms} \tag{63}$$

and

$$\begin{aligned} \tilde{\mathbf{w}}_{m,\text{MV}} &= (\mathbf{Q}_s \mathbf{\Lambda}_s^{-1} \mathbf{Q}_s^H + \mathbf{Q}_n \mathbf{\Lambda}_n^{-1} \mathbf{Q}_n^H) \tilde{\mathbf{a}}_m \\ &= \tilde{\mathbf{w}}_{m,0.5} + \mathbf{Q}_n \mathbf{\Lambda}_n^{-1} \Delta \mathbf{k}_{mn}. \end{aligned} \tag{64}$$

The signal and interference output powers (in direction θ_i) for the two beamformers, respectively, are $p_i G_{\text{T2}}(\theta_i)$ and $p_i G_{\text{MV}}(\theta_i)$, where

$$\begin{aligned} G_{\text{T2}}(\theta_i) &= |\mathbf{a}_i^H \tilde{\mathbf{w}}_{m,0.5}|^2 \\ &= |\mathbf{k}_i^H \mathbf{Q}_s^H (\mathbf{Q}_s \mathbf{\Lambda}_s^{-1} \mathbf{k}_m + \mathbf{Q}_s \mathbf{\Lambda}_s^{-1} \Delta \mathbf{k}_{ms})|^2 \\ &= |\mathbf{k}_i^H \mathbf{\Lambda}_s^{-1} \mathbf{k}_m + \mathbf{k}_i^H \mathbf{\Lambda}_s^{-1} \Delta \mathbf{k}_{ms}|^2 \end{aligned} \tag{65}$$

and

$$\begin{aligned} G_{\text{MV}}(\theta_i) &= |\mathbf{a}_i^H \tilde{\mathbf{w}}_{m,\text{MV}}|^2 \\ &= |\mathbf{k}_i^H \mathbf{\Lambda}_s^{-1} \mathbf{k}_m + \mathbf{k}_i^H \mathbf{\Lambda}_s^{-1} \Delta \mathbf{k}_{ms}|^2. \end{aligned} \tag{66}$$

From (65) and (66), therefore, the signal and interference powers at the output of the T2 and MV beamformers are identical.

The noise power at the output of each beamformer is simply the square of the Euclidean norm of the array weight vector scaled with σ^2. Thus, using (63), the noise power at the output of T2

beamformer is

$$N_{\text{T2}} = \sigma^2 \tilde{\mathbf{w}}_{m,0.5}^{\text{H}} \tilde{\mathbf{w}}_{m,0.5}. \tag{67}$$

Similarly, using (64) the noise power at the output of the MV beamformer is

$$N_{\text{MV}} = \sigma^2 \tilde{\mathbf{w}}_{m,\text{MV}}^{\text{H}} \tilde{\mathbf{w}}_{m,\text{MV}} = N_{\text{T2}} + \frac{1}{\sigma^2} \Delta \mathbf{k}_{mn}^{\text{H}} \Delta \mathbf{k}_{mn} \tag{68}$$

Comparing (67) and (68), since $\Delta \mathbf{k}_{mn}^{\text{H}} \Delta \mathbf{k}_{mn}$ is a non-negative term, we have $\Delta \text{SINR}_{\text{o,T2}} \leqslant \Delta \text{SINR}_{\text{o,MV}}$. Thus

$$\mathscr{S}_{\text{SINR}_{\text{o}},\mathbf{a}}^{\tilde{\mathbf{w}}_{m,0.5}} \leqslant \mathscr{S}_{\text{SINR}_{\text{o}},\mathbf{a}}^{\tilde{\mathbf{w}}_{m,\text{MV}}}. \tag{69}$$

Using (67) and (68), a smaller noise power in the T2 beamformer with constant signal and interference powers induces smaller average sidelobes as compared to the MV beamformer.

Appendix B. Proof of Theorem 4

Assume that there is an uncertainty in $\mathbf{a}_m$ and represent its estimate by $\tilde{\mathbf{a}}_m$ (62). Similar to the Proof of Theorem 3, it can be shown that the array output SNR for the T3 beamformer is

$$\begin{aligned}
\text{SNR}_{\text{o,T3}} &= \frac{p_m G_{\text{T3}}(\theta_m)}{N_{\text{T3}}} \\
&= \text{SNR}_i \frac{|\mathbf{k}_m^{\text{H}} \mathbf{k}_m + \mathbf{k}_m^{\text{H}} \Delta \mathbf{k}_{ms}|^2}{\sigma^2 N_{\text{T3}}}. \tag{70}
\end{aligned}$$

Similarly, the array output SNR of the conventional beamformer is

$$\begin{aligned}
\text{SNR}_{\text{o,C}} &= \frac{p_m G_{\text{C}}(\theta_m)}{N_{\text{C}}} \\
&= \text{SNR}_i \frac{|\mathbf{k}_m^{\text{H}} \mathbf{k}_m + \mathbf{k}_m^{\text{H}} \Delta \mathbf{k}_{ms}|^2}{\sigma^2 N_{\text{T3}} + \Delta \mathbf{k}_{mn}^{\text{H}} \Delta \mathbf{k}_{mn}}. \tag{71}
\end{aligned}$$

Since $\Delta \mathbf{k}_{mn}^{\text{H}} \Delta \mathbf{k}_{mn}$ is a non-negative term, we have $\Delta \text{SNR}_{\text{o,T3}} \leqslant \Delta \text{SNR}_{\text{o,C}}$. Thus

$$\mathscr{S}_{\text{SNR}_{\text{o}},\mathbf{a}}^{\tilde{\mathbf{w}}_{m,0}} \leqslant \mathscr{S}_{\text{SNR}_{\text{o}},\mathbf{a}}^{\tilde{\mathbf{w}}_{m,\text{C}}}. \qquad \square \tag{72}$$

References

[1] A.P. Applebaum, D.J. Chapman, Adaptive array with main beam constraints, IEEE Trans. Antennas Propag. 24 (5) (September 1976) 650–662.

[2] B. Champagne, Q.-G. Liu, Plane rotation-based EVD updating schemes for efficient subspace tracking, IEEE Trans. Signal Process. 46 (7) (July 1998) 1886–1900.

[3] A.C. Chang, C.T. Chiang, Y.H. Chen, A generalized eigenspace-based beamformer with robust capabilities, in: Proceedings of the IEEE International Conference Phase Array Systems Technology, 21–25 May 2000, pp. 553–556.

[4] H. Cox, R.M. Zeskind, M.M. Owen, Robust adaptive beamforming, IEEE Trans. Acoust. Speech Signal Process. 35 (October 1987) 1365–1378.

[5] A. Farina, Antenna-Based Signal Processing Techniques for Radar Systems, Artech House Inc., 1992.

[6] B. Friedlander, A signal subspace method for adaptive interference cancellation, IEEE Trans. Acoust. Speech Signal Process. 36 (12) (December 1988) 1845–1853.

[7] J.D. Gibson (Editor-in-Chief), The Mobile Communications Handbook, CRC Press, Boca Raton, FL, 1996.

[8] A.M. Haimovich, The eigencanceler: adaptive radar by eigenanalysis method, IEEE Trans. Aerospace Electronic Systems 32 (2) (April 1996) 532–542.

[9] H. Krim, M. Viberg, Two decades of array signal processing research, IEEE Signal Process. Mag. (July 1996) 67–94.

[10] C.C. Lee, J.H. Lee, Eigenspace-based adaptive array beamforming with robust capabilities, IEEE Trans. Antennas Propag. 45 (December 1997) 1711–1716.

[11] D. Madurasinghe, An adaptive nulling system for a narrow-band signal with a look Direction constraint using one or more signal subspace eigenvectors, in: Proceedings of the Fifth International Symposium on Signal Processing and its Applications, Australia, August 22–25, 1999, pp. 885–888.

[12] T. McWhorter, Fast rank-adaptive beamforming, Proceedings of the Sensor Array Multichannel Signal Processing Workshop, 2000, pp. 63–67.

[13] W.G. Najm, Constrained least squares in adaptive imperfect analysis, IEEE Trans. Antennas Propag. 38 (11) (November 1990) 1874–1878.

[14] I.S. Reed, I.D. Mallert, L.E. Brennan, Rapid convergence rates in adaptive arrays, IEEE Trans. Aerospace Electronic Systems 10 (November 1974) 853–863.

[15] B.D. van Veen, K.M. Buckley, Beamforming: a versatile approach to spatial filtering, IEEE ASSP Mag. (April 1988) 4–24.

[16] B. Yang, Projection approximation subspace tracking, IEEE Trans. Signal Process. 41 (1) (January 1995) 95–107.

[17] Z. Yongbo, Z. Shouhong, A modified eigenspace-based algorithm for adaptive beamforming, Proceedings of the 15th International Conference on Signal Processing, vol. 1, 2000, pp. 468–471.

[18] J.L. Yu, C.C. Yeh, Generalized eigenspace-based beamformers, IEEE Trans. Signal Process. 43 (11) (November 1995) 2453–2461.

[19] P.A. Zulch, J.S. Goldstein, J.R. Guerci, I.S. Reed, Comparison of reduced-rank signal processing techniques, Proceedings of the 32nd Asilomar Conference on Signals, Systems, and Computers, vol. 1, May 1–4, 1998, pp. 421–425.